Citation: Molecular Therapy — Methods & Clinical Development (2015) **2,** 15022; doi:10.1038/mtm.2015.22

www.nature.com/mtm

ARTICLE

AAV-mediated *RLBP1* gene therapy improves the rate of dark adaptation in *Rlbp1* knockout mice

Vivian W Choi[1], Chad E Bigelow[1], Terri L McGee[1], Akshata N Gujar[1], Hui Li[1], Shawn M Hanks[1], Joanna Vrouvlianis[1], Michael Maker[1], Barrett Leehy[1], Yiqin Zhang[1], Jorge Aranda[1], George Bounoutas[1], John T Demirs[1], Junzheng Yang[1], Richard Ornberg[2], Yu Wang[2], Wendy Martin[3], Kelly R Stout[3], Gregory Argentieri[4], Paul Grosenstein[4], Danielle Diaz[4], Oliver Turner[4], Bruce D Jaffee[1], Seshidhar R Police[1] and Thaddeus P Dryja[1]

Recessive mutations in *RLBP1* cause a form of retinitis pigmentosa in which the retina, before its degeneration leads to blindness, abnormally slowly recovers sensitivity after exposure to light. To develop a potential gene therapy for this condition, we tested multiple recombinant adeno-associated vectors (rAAVs) composed of different promoters, capsid serotypes, and genome conformations. We generated rAAVs in which sequences from the promoters of the human *RLBP1*, *RPE65*, or *BEST1* genes drove the expression of a reporter gene (green fluorescent protein). A promoter derived from the *RLBP1* gene mediated expression in the retinal pigment epithelium and Müller cells (the intended target cell types) at qualitatively higher levels than in other retinal cell types in wild-type mice and monkeys. With this promoter upstream of the coding sequence of the human *RLBP1* gene, we compared the potencies of vectors with an AAV2 versus an AAV8 capsid in transducing mouse retinas, and we compared vectors with a self-complementary versus a single-stranded genome. The optimal vector (scAAV8-p*RLBP1*-h*RLBP1*) had serotype 8 capsid and a self-complementary genome. Subretinal injection of scAAV8-p*RLBP1*-h*RLBP1* in *Rlbp1* nullizygous mice improved the rate of dark adaptation based on scotopic (rod-plus-cone) and photopic (cone) electroretinograms (ERGs). The effect was still present after 1 year.

Molecular Therapy — Methods & Clinical Development (2015) **2**, 15022; doi:10.1038/mtm.2015.22; published online 8 July 2015

INTRODUCTION

Retinitis pigmentosa (RP) is a group of clinically and genetically heterogeneous retinal degenerations which lead to blindness.[1] One form of RP is due to recessive, null mutations in the retinaldehyde binding protein 1 (*RLBP1*) gene that encodes cellular retinaldehyde-binding protein (CRALBP).[2–5] In youth, while the retina is still functional, patients with *RLBP1*-associated retinitis pigmentosa have abnormally slow dark adaptation: after exposure to daylight, the retinas of young patients require 12–24 hours of dark adaptation to achieve normal or almost-normal electroretinogram (ERG) amplitudes (in comparison, normal human retinas recover maximum ERG amplitudes after at most 45 minutes of dark adaptation).[6] Middle-aged and elderly patients typically have severe loss of vision due to photoreceptor degeneration. There is currently no cure or treatment for this condition.

CRALBP is expressed in the retinal pigment epithelium (RPE) and in retinal Müller cells. In the RPE, it functions in the visual cycle by serving as a carrier for 11-cis-retinol and 11-cis-retinal, the chromophore of rod and cone opsins that is delivered to photoreceptors.[7] In Müller cells, CRALBP supports recycling of chromophore that helps cone cells to function in high light intensities.[8,9]

Previously characterized *Rlbp1*$^{-/-}$ knockout mice produce 11-cis retinal at a rate 10-fold more slowly than normal, and they have a correspondingly slow rate of dark adaptation.[10] *Rlbp1*$^{-/-}$ mice do not exhibit the retinal degeneration that occurs in patients with *RLBP1* mutations. Nevertheless, the slow dark adaptation of the mice can be valuable for the assessment of potential gene-replacement therapies for *RLBP1*-associated retinitis pigmentosa, as is described in this paper.

RESULTS

Assessment of promoter activities and rAAV genome conformations

We used rAAV vectors with a serotype 8 capsid to test the ability of various promoters and genome configurations to express a transgene specifically in the RPE and the Müller cells, the cells in which CRALBP is normally expressed.[10]

We created vectors carrying a green fluorescent protein (eGFP) gene under the transcriptional control of the following four promoters: (i) p*RLBP1*(short) derived from nucleotides -3,157 through -2,568 upstream of the first base of the translation start codon in exon 3 of the human *RLBP1* gene; (ii) p*RLBP1*(long) derived from nucleotides -3,157 through -1 upstream of the translation start codon of the

[1]Ophthalmology Disease Area, Novartis Institutes for BioMedical Research, Cambridge, Massachusetts, USA; [2]Ophthalmology Disease Area, Novartis Institutes for BioMedical Research, Fort Worth, Texas, USA; [3]Preclinical Safety, Alcon, Fort Worth, Texas, USA; [4]Preclinical Safety, Novartis Institutes for BioMedical Research, East Hanover, New Jersey, USA. Correspondence: VW Choi (vichoi@shire.com)
Received 22 January 2015; accepted 5 May 2015

human *RLBP1* gene; (iii) p*RPE65* derived from base -1,610 through -31 upstream of the translation start codon in exon 1 of the human *RPE65* gene; and (iv) p*BEST1* derived from the nucleotides -2,038 through -1,417 upstream of the translation start codon in exon 2 of the human *BEST1* gene.

Each of these four promoters driving the eGFP gene was engineered into rAAV8 vectors with single-stranded genomes. In addition, the p*RLBP1*(short) promoter was used to create a rAAV8 vector with a self-complementary (also known as double-stranded) genome. Subretinal injections of 1×10^8 or 1×10^9 vg/eye of each of the five vectors transduced the RPE of wild-type mice, with the p*RLBP1*(short), single-stranded vector mediating the lowest apparent expression of eGFP. In contrast, there was robust expression across large areas of RPE mediated by the p*RLBP1*(short), self-complementary vector (Figure 1a). Only the vectors with the p*RLBP1*(short) and the p*RLBP1*(long) promoters transduced Müller cells. Figure 1b through Figure 1h show the expression of eGFP in cells transduced with the self-complementary vector with the *RLBP1*(short) promoter. The vector induced eGFP expression in cells of the inner nuclear layer and in cell processes extending from the external limiting membrane to the end feet of the inner limiting membrane that co-expressed the Müller cell marker CRALBP (Figure 1b–d). Additional confirmation of Müller cell localization was obtained through costaining of eGFP with vimentin (Figure 1e–g) and GFAP (Figure 1h), which both detect intermediate filaments located in the end feet and inner retinal processes of Müller cells.[11] Off-target eGFP expression in cone photoreceptors determined through colocalization of eGFP with blue or green cone opsins was found with the vectors with the *RLBP1*(long) (not shown), *RPE65* (Figure 1l), and *BEST1* (Figure 1p) promoters but not from the self-complementary vector with the *RLBP1*(short) promoter (Figure 1i–k, m–o). A summary of these qualitative results is shown in Table 1.

To evaluate the promoter p*RLBP1*(short) in the retina of a species closer to humans, doses of 1×10^9 vg/eye of the self-complementary rAAV8 vector scAAV8-p*RLBP1*(short)-eGFP were subretinally injected into both eyes of two Cynomolgus monkeys (*Macaca fascicularis)*. As seen in mice, the RPE around the injection sites expressed eGFP (Figure 1q). In the neural retina, eGFP was also expressed in some cell bodies in the inner nuclear layer with processes spanning from the external limiting membrane to the inner limiting membrane. Even though costaining of cell type-specific markers were not performed, the eGFP-expression pattern was consistent with the anatomical pattern expected for Müller cells and RPE (Figure 1q).

Three of the promoters were further characterized in mice by evaluating four rAAV8 vectors in which the promoters drove the expression of a cDNA sequence derived from the human *RLBP1* gene: one with the p*RLBP1*(short) promoter in a single-stranded genome called ssAAV8-p*RLBP1*(short)-h*RLBP1*, one with the p*RLBP1*(short) promoter in a self-complementary genome called scAAV8-p*RLBP1*(short)-h*RLBP1*, one with the p*RLBP1*(long) promoter in a single-stranded genome called ssAAV8-p*RLBP1*(long)-h*RLBP1*, and one with the p*RPE65* promoter in a single-stranded genome called ssAAV8-p*RPE65*-h*RLBP1*. Levels of human *RLBP1* (h*RLBP1*) mRNA were measured in the neural retina and the eye cup (which included the whole eye minus the lens and neural retina) four weeks after subretinal injections of 1×10^8 or 1×10^9 vg/eye in wild-type mice. At a dose of 1×10^9 vg/eye (Figure 2a) of the self-complementary vector with the short *RLBP1* promoter, scAAV8-p*RLBP1*(short)-h*RLBP1*, had the highest expression in the neural retina and the eye cup. At a 10-fold lower dose of 1×10^8 vg/eye (Figure 2b), the only vector that showed substantial expression levels of the h*RLBP1* transgene in neural retina was scAAV8-p*RLBP1*(short)-h*RLBP1*. This vector also produced the highest level of h*RLBP1* transgene expression in the eye cup at a dose of 1×10^8 vg/eye. Due to its higher transduction efficiency and cell-specific expression pattern, this self-complementary rAAV8 vector with the short *RLBP1* promoter (scAAV8-p*RLBP1*(short)-h*RLBP1*) was chosen for subsequent efficacy studies in mice.

Characterization of nullizygous *Rlbp1* mice

The Lexicon mouse line TF0133 used in this research has a 496-bp deletion that begins in exon 3 and extends to the end of exon 4. The deletion removes the initiation methionine codon in exon 3 (Figure 3a). PCR using primers that straddle the deletion breakpoints amplified fragments from genomic DNA of *Rlbp1*$^{+/+}$, *Rlbp1*$^{+/-}$, and *Rlbp1*$^{-/-}$ mice that corresponded in length to the presence or absence of the deletion (Figure 3b). The mutation creates a null allele, as confirmed through analysis of CRALBP protein. Specifically, the rabbit polyclonal anti-CRALBP antibody (15356-1-AP) detected CRALBP in wild-type mice in both the RPE and in the neural retina. The pattern of staining in the neural retina indicated that CRALBP was in Müller cell bodies, processes, and end feet (Figure 3c). No CRALBP was detected in the neural retina or the RPE in *Rlbp1*$^{-/-}$ mice (Figure 3d). The thickness of the retina of *Rlbp1*$^{+/+}$ mice and *Rlbp1*$^{-/-}$ mice was measured at 4, 10, and 16 months of age. There was no detectable reduction in retinal thickness up to 16 months of age (Figure 3e,f).

Similar to young patients with *RLBP1*-associated retinitis pigmentosa prior to substantial retinal degeneration, after long periods of dark adaption (*e.g.*, ≥24 hours), the ERGs of *Rlbp1*$^{-/-}$ mice had normal amplitudes in response to single flashes of light.[10] However, after bleaches of more than 10% of rhodopsin, *Rlbp1*$^{-/-}$ mice required many hours of dark adaptation to regain full light sensitivity, in contrast to the substantial recovery observed in only about 3 hours in *Rlbp1*$^{+/+}$ mice.[10] Figure 4a,b illustrates the difference in ERG amplitudes between *Rlbp1*$^{-/-}$ and *Rlbp1*$^{+/+}$ mice after 4 hours of dark adaptation as compared with the fully dark-adapted responses of each mouse. *Rlbp1*$^{+/+}$ mice exhibit nearly full recovery of scotopic visual function (as indicated by a-wave amplitudes) in contrast to *Rlbp1*$^{-/-}$ mice which have minimal recovery. This slow dark adaptation is in qualitative agreement with results reported previously in *Rlbp1*$^{-/-}$ mice with a different null mutation.[10]

The vector scAAV8-p*RLBP1*(short)-h*RLBP1* expresses CRALBP *in vivo*

The mouse monoclonal anti-CRALBP antibody (sc59487) was used to qualitatively determine whether the vector scAAV8-p*RLBP1*(short)-*hRLBP1* mediated CRALBP expression in mouse retina. The antibody detected CRALBP in neural retinal lysates from *Rlbp1*$^{-/-}$ mouse eyes injected with 1×10^9 vg of scAAV8-p*RLBP1*(short)-h*RLBP1* (Figure 3g). As negative and positive controls, respectively, equal amounts of protein from the neural retinal lysates of untreated *Rlbp1*$^{-/-}$ mice had no detected CRALBP protein, while lysates from wild-type mice had CRALBP. The absence of CRALBP detected in lysates was in accord with its not being detected in histologic sections, as mentioned above (Figure 3d). Technical challenges were encountered when analyzing by Western blotting the protein lysates generated from tissue containing RPE. However, RPE transduction was indirectly suggested by functional rescue described below.

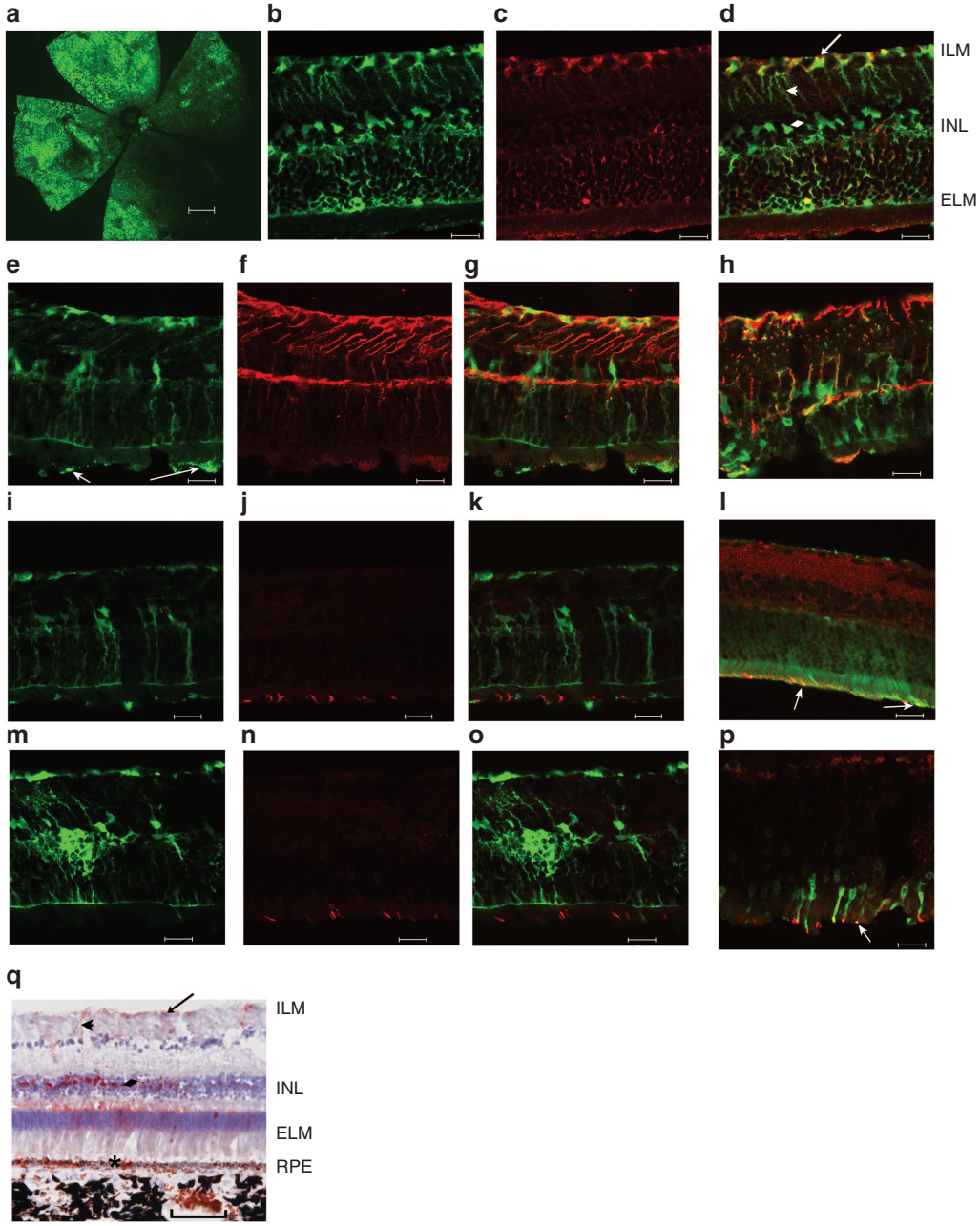

Figure 1 Patterns of eGFP expression mediated by reporter vectors in mouse and monkey retinas. (**a**) Following dissection of the neural retina from a mouse eye injected with scAAV8p*RLBP1*(short)-eGFP, the remaining eye cup was fixed, flat-mounted and imaged. The photograph shows the large geographic regions of RPE that express eGFP. (**b–p**) Neural retina was fixed, sectioned and costained with cell-specific antibody markers. (**b–d**) Images of a retina transduced by the scAAV8-p*RLBP1*(short)-eGFP vector showing eGFP, CRALBP, and the merger of eGFP and CRALBP signals demonstrate eGFP expression in CRALBP-expressing Müller cells spanning the retina from the external limiting membrane to the end feet in the inner limiting membrane; (**e–h**) eGFP, vimentin, eGFP+vimentin merged, and eGFP+GFAP merged indicate that eGFP is coexpressed with vimentin and GFAP in Müller cell processes of the inner nuclear layer and the inner limiting membrane where vimentin and GFAP are in intermediate filaments of Müller cells. (**i–k**) Images of eGFP, blue opsin, and eGFP+blue opsin merged reveal that eGFP does not colocalize with cone photoreceptors that express blue opsin, and (**m–o**) images of eGFP, green opsin, and eGFP+green opsin merged show that eGFP does not colocalize with cone photoreceptors that express green opsin. As examples of off-target photoreceptor expression, images from a (**l**) merger of images of eGFP+blue opsin expression from a retina injected with ssAAV8-p*BEST*-eGFP injected eye show colocalization of eGFP and blue opsin indicated by the two white arrows, and (**p**) a merger of images of eGFP+green opsin staining from an ssAAV8-p*RPE65*-eGFP injected eye reveals colocalization of eGFP expression and green opsin. (**q**) Immunohistochemistry (red peroxidase stain) with an anti-eGFP antibody on a monkey eye that had been previously injected with a scAAV8-pRLBP1(short)-eGFP vector was performed on paraffin sections through the transduced region of the eye to visualize the vector-mediated expression of eGFP. Cells with the red peroxidase stain have nuclei in the inner nuclear layer and processes that extend from the inner limiting membrane to the external limiting membrane, consistent with their identity as Müller cells. Mouse eyes were harvested 4 weeks after subretinal injection of the reporter vectors; monkey eyes were harvested 71 days after subretinal injection. ELM, external limiting membrane; ILM, inner limiting membrane; INL, inner nuclear layer; RPE, retinal pigment epithelium; diamond, cell bodies of INL; arrowhead, Müller cell processes; arrow (**d+q**), Müller cell end feet; asterisk, staining in RPE; arrow (**e**), retained RPE tissue; arrow (**l+p**) positive co-stained cells; Scale bars, 500 µm in **a**, 20 µm in **b-p**, and 100 µm in **q**.

Table 1 Cell localization of AAV8-mediated eGFP expression driven by different promoters

		Vector injected subretinally at 1 × 10⁹ vg/eye			
Cell type	[b]*Cell marker*	*scAAV8-pRLBP1(short)-eGFP*	*ssAAV8-pRLBP1 (long)-eGFP*	*ssAAV8-pRPE65-eGFP*	*ssAAV8-pBEST1-eGFP*
[a]RPE		POS	POS	POS	POS
Müller cells	CRALBP	POS	POS	NEG	NEG
	Vimentin	POS	POS	NEG	NEG
	GFAP	POS	POS	NEG	NEG
Photoreceptors	Green Opsin	NEG	[c]POS	[c]POS	[c]POS
	Blue Opsin	NEG	NEG	[c]POS	[c]POS
Neurons in INL	PKCα	NEG	NEG	NEG	NEG
Ganglion cells	NeuN	NEG	ND	ND	ND
Astrocytes	GFAP	NEG	NEG	NEG	NEG

ND, not determined.
[a]Flatmounts of posterior eye cups from injected wild-type mouse eyes were scored positive for a detected presence of eGFP. [b]eGFP-positive neural retinas were sectioned and stained using specific retina cell marker antibodies to confirm cell type where eGFP was expressed. [c]Represents off-target expression

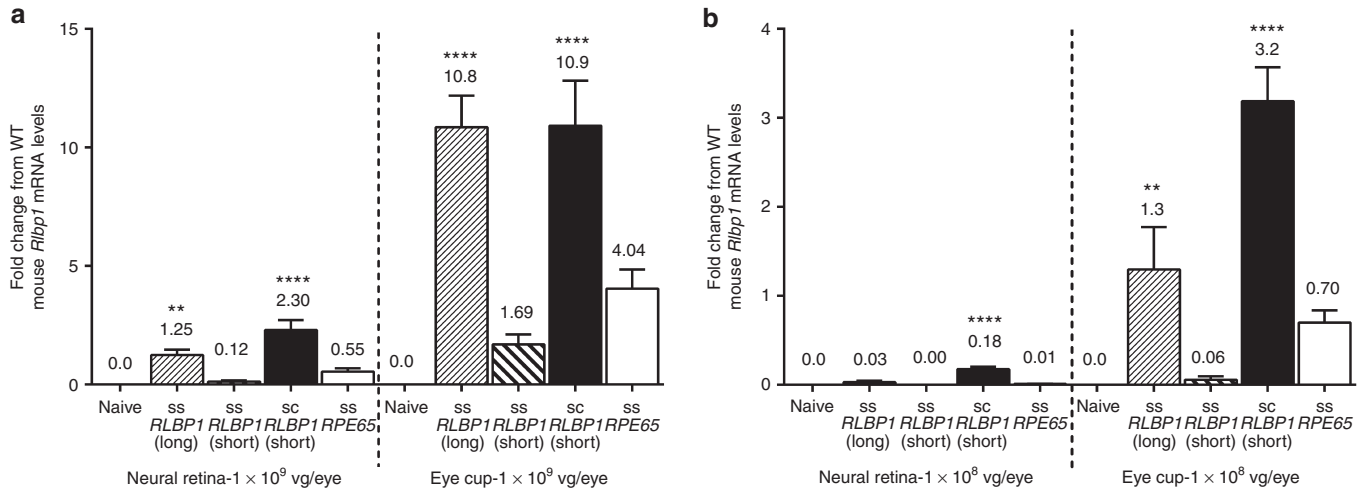

Figure 2 Vector mediated expression levels of the human *RLBP1* transgene under the transcriptional control of different promoters. (**a,b**) Relative mRNA levels of vector-mediated *RLBP1* expression were assayed using qPCR probes specific for human *RLBP1* or mouse *Rlbp1* and RNA extracted from wild-type mouse neural retina or eye cups 4 weeks after subretinal injection with rAAV vectors carrying different promoters or genome conformations driving h*RLBP1* expression. Relative expression of *RLBP1* is graphed as a mean fold change from WT mouse *Rlbp1* expression +SEM. Naive (uninjected) neural retina (nr) and eye cup (ec) samples were also included at each dose ($n = 12$). (**a**) Relative *RLBP1* expression mediated by a dose of 1×10^9 vg/eye of vectors ssAAV8-p*RLBP1*(long)-h*RLBP1* (nr $n = 20$; ec $n = 17$), ssAAV8-p*RLBP1*(short)-h*RLBP1* (nr+ec $n = 8$), scAAV8-p*RLBP1*(short)-h*RLBP1* (nr $n = 19$; ec $n = 16$), or ssAAV8-p*RPE65*-h*RLBP1* (nr $n = 19$; ec $n = 15$). (**b**) Relative *RLBP1* expression mediated by a dose of 1×10^8 vg/eye of vectors ssAAV8-p*RLBP1*(long)-h*RLBP1* (nr $n = 9$; ec $n = 7$), ssAAV8-p*RLBP1*(short)-h*RLBP1* (nr+ec $n = 4$), scAAV8-p*RLBP1*(short)-h*RLBP1* (nr+ec $n = 9$), or ssAAV8-p*RPE65*-h*RLBP1* (nr+ec $n = 8$). WT, wild-type; ss, single-stranded vector genome; sc, self-complementary vector genome. Calculations of *P* values compared expression levels to naive wild-type eyes; $^{**}P \leq 0.01$; $^{****}P \leq 0.0001$.

The scAAV8-p*RLBP1*(short)-h*RLBP1* vector improves dark adaptation in *Rlbp1*$^{-/-}$ mice

In *Rlbp1*$^{-/-}$ mouse eyes treated 50 weeks earlier with a subretinal injection of 3.5x10^8 vg/eye of the vector scAAV8-p*RLBP1*(short)-h*RLBP1* (abbreviated as AAV8), the ERG a-wave amplitude 4 hours after bleach was 64% of the maximum amplitude achieved after overnight dark adaptation. In contrast, untreated *Rlbp1*$^{-/-}$ mice exhibited minimal recovery of the a-wave 4 hours after bleach (Figure 4c,d).

We explored the dose-response relationship of the vector by administering subretinal doses of 3×10^6, 3×10^7, 3×10^8, and 1×10^9 vg/eye. For comparison, negative controls included naive mice as well as mice that received injections of a null rAAV8 vector carrying no transgene at a dose of 1×10^9 vg/eye. After four hours of dark adaptation, mouse eyes that had received scAAV8-p*RLBP1*(short)-h*RLBP1* at doses of 3×10^8 and 1×10^9 vg/eye had ERG amplitudes 69 and 85%, respectively, of the maximum amplitudes achieved after overnight dark adaptation. The a-wave recoveries of these eyes were

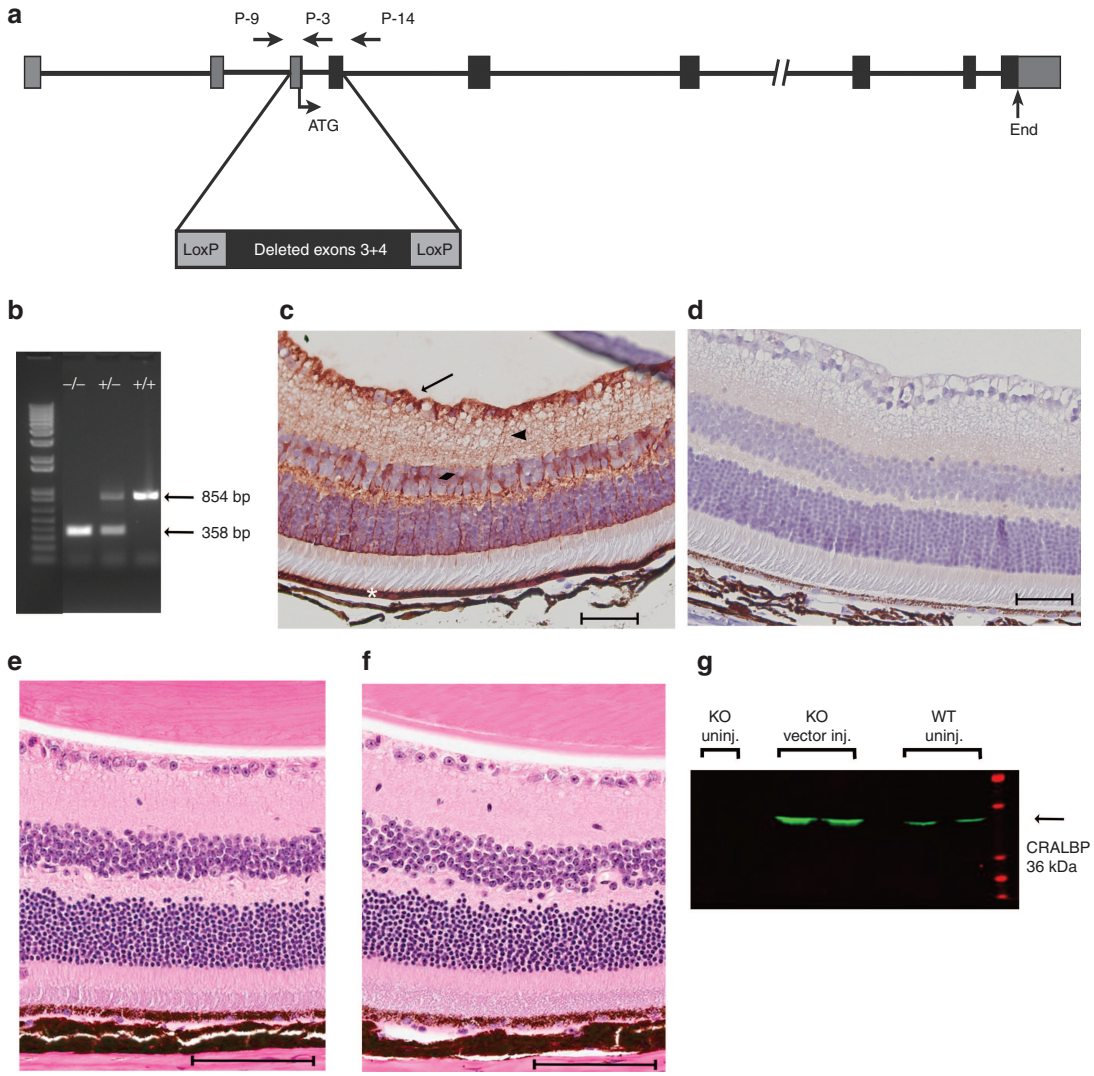

Figure 3 Characterization of the *Rlbp1*$^{-/-}$ mouse. (**a**) The horizontal bar is a schematic representation of the *Rlbp*1 targeted deletion in the Lexicon TF0133 mouse line. Primers used for genotyping are depicted as arrows (P-9, P-3, and P-14). (**b**) PCR analysis of DNA from *Rlbp1*$^{-/-}$, *Rlbp1*$^{+/-}$, and *Rlbp1*$^{+/+}$ mice using primers P-9, P-3, and P-14 show the expected 854 bp amplicon of the WT allele and the 358 bp amplicon of the allele carrying the deletion. (**c,d**) Paraffin sections of *Rlbp1*$^{+/+}$ (**c**) and *Rlbp1*$^{-/-}$ (**d**) mouse eyes stained with an antibody against CRALBP. (**e,f**) Hematoxylin and eosin stained paraffin sections of 16-month-old *Rlbp1*$^{+/+}$ (**e**) and *Rlbp1*$^{-/-}$ (**f**) mouse eyes. (**g**) Lysates of neural retina from uninjected *Rlbp1*$^{-/-}$ (KO uninj.), *Rlbp1*$^{-/-}$ injected with 1×10^9 vg/eye of scAAV8-p*RLBP1*(short)-h*RLBP1* (KO, vector inj.), and uninjected *Rlbp1*$^{+/+}$ (WT uninj.) mice were analyzed by western blot using a primary antibody against CRALBP. Arrow, end feet of Müller cells; arrow head, Müller cell processes; diamond, cell bodies of inner nuclear layer; asterisk, RPE; scale bars, 50 µm in **c+d** and 100 µm in **e+f**.

greater than those eyes receiving lower doses, negative control vector, or were untreated (Figure 5).

An AAV serotype 8 capsid vector improves the amplitude of dark adaptation better than an AAV serotype 2 capsid vector

We compared the efficacy of rAAV2 and rAAV8 vectors in *Rlbp1*$^{-/-}$ mice. The self-complementary p*RLBP1*(short)-h*RLBP1* expression cassette was packaged into AAV2 and AAV8 serotype capsids. Vectors were subretinally injected at a dose of 3.5×10^8 vg/eye and the a-wave amplitudes 4 hours after a bleach were measured at several time points after the injections. Both the AAV2 capsid and the AAV8 capsid vectors significantly improved the amplitude of dark adaptation in comparison to untreated (naive) *Rlbp1*$^{-/-}$ mice, but the interval of time between the injection and the onset of significant efficacy differed. With the AAV8 capsid vector, the a-wave recovery improved 2 weeks after the injection versus 12 weeks for the AAV2 capsid vector. In addition, the AAV2 capsid vector mediated significantly less improvement in the ERG amplitude 4 hours after a bleach compared to the AAV8 capsid vector at all time-points measured (Figure 6).

The effects of the vectors persist for a year

The improvements in the rate of dark adaptation after single injections of vectors expressing human CRALBP were long-lasting. In the studies comparing AAV2 and AAV8 capsid serotypes, treated mice that were followed for at least 50 weeks still had, 4 hours after a bleach, ERG amplitudes that were 64% (for the AAV8 capsid vector) and 29% (for the AAV2 capsid vector), of maximal dark-adapted ERG amplitudes (Figure 6). Similarly, mice in the experiments exploring various doses of the scAAV8-p*RLBP1*(short)-h*RLBP1* vector (Figure 5) were followed over time. Approximately one year after the injections, eyes receiving 3×10^8 or 1×10^9 vg/eye still had improved ERG amplitudes 4 hours after a bleach (data not shown).

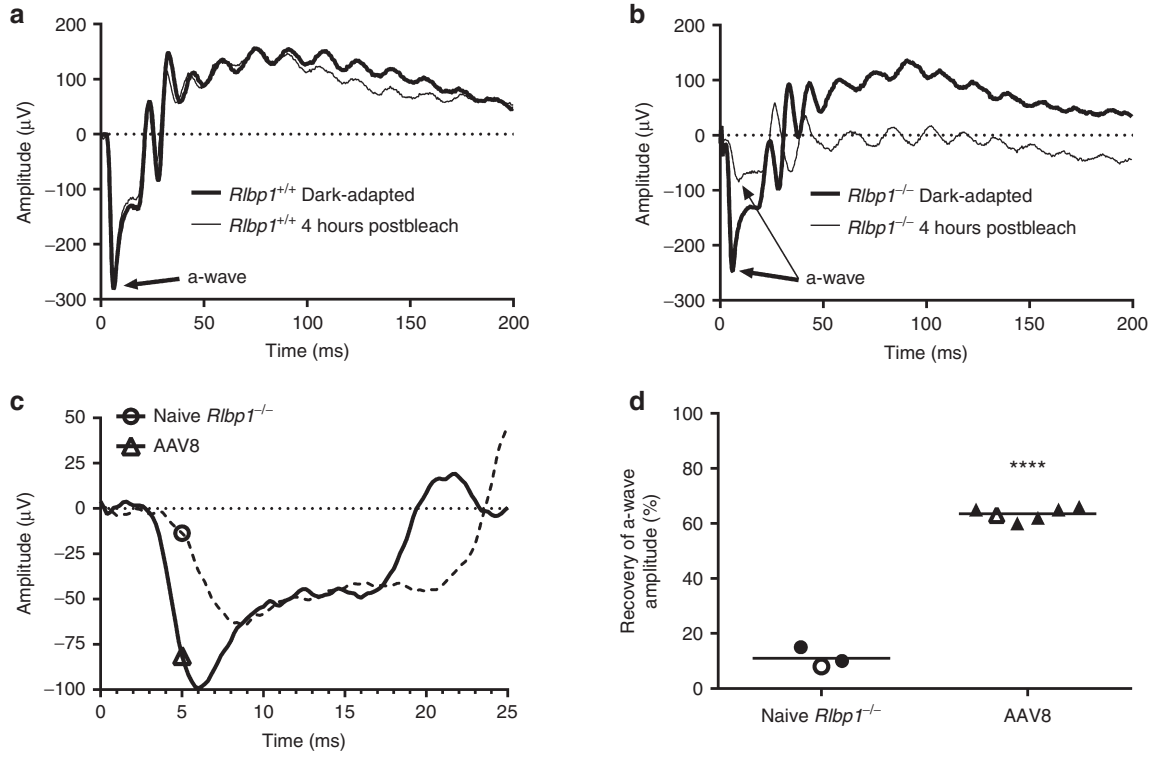

Figure 4 Vector-mediated improvement of dark adaptation in *Rlbp1*$^{-/-}$ mice. (**a–d**) ERGs were measured in mice fully dark-adapted overnight (>15 hours) to obtain responses to a single intensity white light flash. Following another overnight dark adaptation, mice were exposed to a bleaching light, dark adapted for 4 hours and ERGs were remeasured. (**a,b**) ERG traces are shown from (**a**) 70-week-old naive *Rlbp1*$^{+/+}$ and (**b**) 68-week-old naive *Rlbp1*$^{-/-}$ mice recorded in conjunction with the week 50 postinjection measurement shown in Figure 6. The maximum responses after full dark adaptation are shown as bold lines while responses 4 hours following a photobleach are shown as thin lines. Arrows point to the a-wave of the ERG responses. (**c**) ERGs from naive and treated *Rlbp1*$^{-/-}$ mice 4 hours following a photobleach. The recordings were performed 50 weeks postsubretinal injection. Note that the time scale is expanded compared to (**a**) and (**b**). The open triangle (treated) and open circle (naive) symbols indicate the time after a flash (5 milliseconds) at which we measured amplitudes. (**d**) The graph contains 50-week postinjection a-wave recovery data (dark adaptation) from all tested mice achieved by dividing the a-wave amplitude 4 hours postphotobleach in each eye by its respective maximum dark-adapted value (same data set as presented in Figure 6, 50-week time point for AAV8 vector treated and naive eyes). Open symbols in (**d**) correspond to data from the traces in (**c**). Each symbol represents 1 eye of each mouse tested. AAV8, subretinally injected with scAAV8-p*RLBP1*(short)-h*RLBP1*. Calculations of *P* values compare treated eyes to naive *Rlbp1*$^{-/-}$ eyes. ****$P \leq 0.0001$.

Cone-driven ERG responses were restored by the scAAV8-p*RLBP1*(short)-h*RLBP1* vector

We explored cone-driven ERG responses in *Rlbp1*$^{+/+}$ and *Rlbp1*$^{-/-}$ mice to assess whether a measurable difference in function could be detected as described in a previous publication involving mice with a different null mutation of *Rlbp1*.[10] Like the mice in the previous publication, our *Rlbp1*$^{-/-}$ mice had cones that more slowly dark-adapted compared to *Rlbp1*$^{+/+}$ controls, although the kinetics were different from what was described in the previously published strain. Photopic ERGs did not differ between our *Rlbp1*$^{-/-}$ and *Rlbp1*$^{+/+}$ mice after overnight dark adaptation (data not shown). Immediately after bleaching with a 1200 cd (photopic) white LED light for one minute, photopic b-wave amplitudes of wild-type mice were reduced, but they recovered to 55–60% of the baseline value within 2.5–5 minutes (Figure 7a,d). In contrast, cone-mediated b-wave amplitudes from *Rlbp1*$^{-/-}$ mice did not detectably recover during the first 20 minutes after a bleach (Figure 7b,d). Ten weeks after subretinal injection of 1×10^9 vg of the self-complementary vector scAAV8-p*RLBP1*(short)-h*RLBP1*, *Rlbp1*$^{-/-}$ mice had rapid recovery kinetics similar to that observed in *Rlbp1*$^{+/+}$ mice (Figure 7c,d), indicating that the vector restored rapid cone adaptation in *Rlbp1*$^{-/-}$ mice.

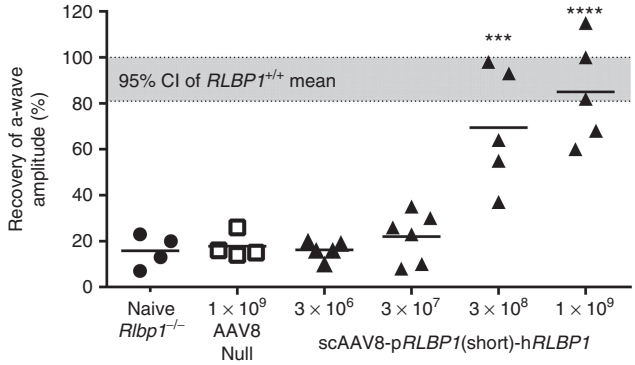

Figure 5 Dose–response relationship of a-wave recoveries in *Rlbp1*$^{-/-}$ mice treated with scAAV8-p*RLBP1*(short)-h*RLBP1*. Data points represent a-wave recoveries of individual mouse eyes (1 eye per mouse) assessed 12 or 13 weeks postsubretinal delivery of 3×10^6, 3×10^7, 3×10^8, or 1×10^9 vg/eye of scAAV8-p*RLBP1*(short)-h*RLBP1* or 1×10^9 vg/eye of a null vector. The 95% confidence interval (CI) of the mean from several cohorts of *Rlbp1*$^{+/+}$ mice is represented by the shaded region ($n = 23$ eyes). Calculations of p-values compare treated eyes to naive *Rlbp1*$^{-/-}$ eyes. ***$P \leq 0.001$; ****$P \leq 0.0001$.

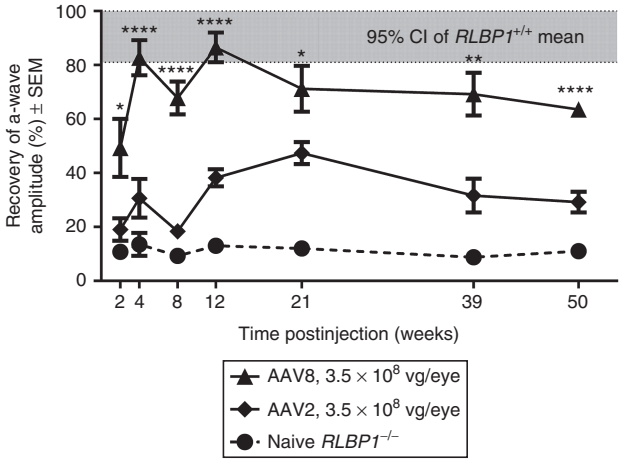

Figure 6 Comparison of scAAV8-p*RLBP1*(short)-h*RLBP1* versus scAAV2-p*RLBP1*(short)-h*RLBP1* in a year-long longitudinal study. The recovery of the a-wave amplitude was measured in mice injected with 3.5×10^8 vg/eye of either scAAV8-p*RLBP1*(short)-h*RLBP1* ($n = 6$ eyes) or scAAV2-p*RLBP1*(short)-h*RLBP1* (n=5 eyes) at time points ranging from 2 to 50 weeks postinjection. ERGs were also measured from naive *Rlbp1*$^{-/-}$ mice which served as negative controls ($n = 3$–4 mice). Data are graphed as percent recovery of the a-wave amplitude ± SEM. The 95% confidence interval (CI) of the mean from several cohorts of *Rlbp1*$^{+/+}$ mice is represented by the shaded region ($n = 23$ eyes). Mice receiving AAV8-capsid vector exhibited substantial a-wave recovery compared to naive controls at 2 weeks ($P \le 0.05$), 4 weeks ($P \le 0.0001$), 8 weeks ($P \le 0.0001$), 12 weeks ($P \le 0.0001$), 21 weeks ($P \le 0.001$), 39 weeks ($P \le 0.001$), and 50 weeks ($P \le 0.0001$) postinjection. Recovery was detected starting at 12 weeks postinjection with the AAV2-capsid vector-injected eyes compared to naive controls ($P \le 0.01$, $P \le 0.01$, $P \le 0.05$, $P \le 0.001$ for the respective timpoints on the graphs from weeks 12 to 50). The *P* values for the comparison between AAV8-capsid and AAV2-capsid vector-injected groups within each time point are displayed in the figure. *$P \le 0.05$; **$P \le 0.01$; ****$P \le 0.0001$.

DISCUSSION

The goal of this study was to design an AAV-based gene therapy for *RLBP1*-associated retinitis pigmentosa. For this purpose, we sought a vector that would preferentially transduce the RPE and Müller cells, the two retinal cell types that normally express *RLBP1*.[12] In reports of AAV-based gene therapy for *RPE65*-associated retinal degeneration, the *RPE65* transgene was driven by the ubiquitously active chicken β-actin promoter.[13–15] Even if there were unintended expression of RPE65 in cells other than the RPE, it would likely not have a negative impact, because the substrate of RPE65, all-trans retinyl ester, is found in RPE cells but not in other cell types in the retina. In contrast, the 11-cis retinoids that form complexes with CRALBP are in photoreceptors as well as the RPE and Müller cells. If CRALBP were aberrantly expressed in photoreceptors, it might compete with opsins for chromophore. For these reasons, we believe that it was important to limit *RLBP1* expression to only the RPE and Müller cells.

We explored different serotypes and promoters to find a vector with the required expression pattern. We chose the AAV8 capsid because it was shown previously to transduce cells in monkey retinas at lower doses than required for AAV2 capsid.[16] In addition, at the dose of 3.5×10^8 vg/eye, we demonstrated that the scAAV8-p*RLBP1*(short)-h*RLBP1* vector mediated significantly better improvement in the ERG recovery compared with the corresponding AAV2 capsid vector at all time-points measured through 50 weeks. Among the promoters we tested, a 590 bp DNA fragment derived from the human *RLBP1* promoter directed the expression of transgenes specifically to the RPE and Müller cells. In contrast, a 3,157-bp fragment derived from the 5′ human *RLBP1* gene sequence directed expression not only to the RPE and Müller cells but also to the photoreceptors. Promoter fragments derived from the *RPE65* or *BEST1* genes directed expression mainly in the RPE and photoreceptors with minimal to no expression in Müller cells. Based on these results, the most suitable vector was composed of the AAV serotype 8 capsid and carried a 590 bp *RLBP1* fragment (called *pRLBP1*(short)) as the promoter.

We created two vectors having the AAV8 capsid and the *pRLBP1*(short) promoter driving the human *RLBP1* coding sequence: one vector, called ssAAV8-p*RLBP1*(short)-h*RLBP1,* had a single stranded genome and the other vector, called scAAV8-p*RLBP1*(short)-h*RLBP1,* had a self-complementary (double-stranded) genome. We found that the vector with the self-complementary genome was more potent; *i.e.*, a given dose induced greater transgene expression in the retina. The higher potency of vector with AAV8 capsid and a self-complementary versus a single-stranded genome is in agreement with previously published experiments that compared the two genome conformations.[17] A scAAV8 vector with the short *RLBP1* promoter driving a reporter gene retained the ability to specifically transduce the RPE and Müller cells when injected subretinally in monkey eyes.

Two weeks after a subretinal injection of scAAV8-p*RLBP1*(short)-h*RLBP1* in *Rlbp1*$^{-/-}$ mice, there was detectable improvement in the rate of dark adaptation, as measured by ERG a-wave recovery after a bleaching light (Figure 6). By 1–3 months after an injection, the rate of dark adaptation was normal or close-to-normal (Figures 5 and 6). The improvement was dose-dependent, with a dose of 3×10^7 vg/eye having no significant effect and doses of 3×10^8 vg/eye and 1×10^9 vg/eye having a progressively greater effect (Figure 5). The improvement in the rate of dark adaptation persisted for at least 50 weeks after a single injection (Figure 6).

We saw some variability in the a-wave recovery between mice injected with the same dose of vector and in mice over time. Some of the variability between treated mouse eyes may be due to variability in the area of vector-containing bleb or leakage of the test article into the vitreous during subretinal delivery. Since the full-field ERG is an average of the response across the entire retina, the a-wave recovery would depend in part on the fraction of retina transduced. Full-field ERGs might underestimate the actual physiologic improvement in the transduced regions of retina because an injection typically transduce only about 60–80% of the retinal area.[18] Another source of variability is from the method of recording ERGs. There is substantial test-retest variability, and our calculation of dark adaptation relies upon the division of two ERG measurements: the amplitude after 4 hours of dark adaptation divided by the amplitude after overnight dark adaptation. We tried to minimize this variability by retaining the same operators as much as feasible through each longitudinal study.

The ERG a-waves that we routinely recorded reflect predominantly rod function. In separate recording sessions we modified the ERG protocol to detect cone-dominated signals. After a bleaching light, the cone ERG amplitude in wild-type mice increased within 5 minutes to about 55–60% of the pre-bleach amplitude, and there was minimal if any increase over the next 15 minutes. We were uncertain of the reason for incomplete b-wave recovery in wild-type mice during the first 20 minutes after a bleach. Since ERG cone recordings require a total of 70 rod-saturating stimuli as part of the paired-flash protocol, incomplete cone b-wave recovery could be due a bleaching effect from the cumulative flashes. Alternatively, it is possible that the recovery observed in the

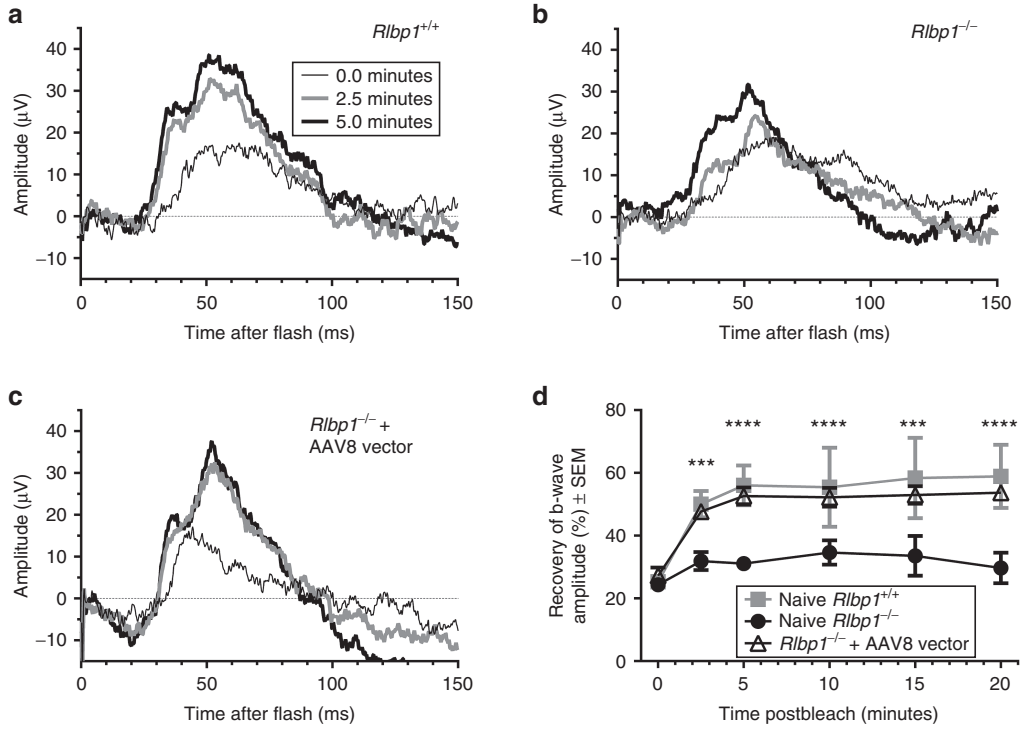

Figure 7 scAAV8-p*RLBP1*(short)-h*RLBP1* improves cone dark adaptation in *Rlbp1*$^{-/-}$ mice. (**a–c**) Cone-driven ERG-responses were extracted by the measurement of b-wave amplitudes from a paired-flash protocol at various time points following a 1 minute photobleach. Representative ERG traces from the paired-flash protocol at 0.0, 2.5, and 5.0 minutes post-bleach in *Rlbp1*$^{+/+}$ mice, *Rlbp1*$^{-/-}$ mice, and *Rlbp1*$^{-/-}$ mice treated with a subretinal injection scAAV8-p*RLBP1*(short)-h*RLBP1* 10 weeks prior to recordings are shown (**a–c** respectively). (**d**) The graph displays average b-wave recoveries normalized to dark-adapted pre-bleach levels in *Rlbp1*$^{+/+}$ ($n = 4$), *Rlbp1*$^{-/-}$ ($n = 3$), and vector treated *Rlbp1*$^{-/-}$ ($n = 9$) mice. The *P* values displayed in the plot compare the b-wave recovery at the 0 minute time point to later time points within the AAV8 vector-treated group (***$P \leq 0.001$; ****$P \leq 0.0001$). Analysis was also performed to compare recoveries between groups at each time point (not displayed in the plot). This comparison indicates significant recovery in naive *Rlbp1*$^{+/+}$ mice and *Rlbp1*$^{-/-}$ mice receiving AAV8 vector compared to naive *Rlbp1*$^{-/-}$ mice at 2.5, 5, and 20 minutes postbleach (naive *Rlbp1*$^{+/+}$: $P \leq 0.05$, $P \leq 0.01$, $P \leq 0.05$; *Rlbp1*$^{-/-}$ + AAV8 vector. $P \leq 0.01$, $P \leq 0.01$, $P \leq 0.01$ for the respective 2.5, 5, and 20 minute time points). No corresponding difference was detected at 0, 10, or 15 minutes ($P > 0.05$). No significant difference was detected between *Rlbp1*$^{+/+}$ and *Rlbp1*$^{-/-}$ + AAV8 vector groups at any time point.

first 5 minutes reflects the Müller cell-mediated regeneration of chromophore and that complete recovery requires more than 20 minutes due to its dependence on the slower, canonical chromophore regeneration in the RPE. This is consistent with the findings of Kolesnikov *et al*.[19] in which mouse M/L cone dark adaptation was bi-phasic with a fast initial recovery dependent on a process internal to the neural retina and a second, slower recovery dependent on the RPE. It is plausible that the vector restored both the neural-retina-mediated and RPE-mediated visual cycles by transducing the Müller cells and the RPE cells, respectively, but that 20 minutes was insufficient for complete recovery. Regardless of the reason for the incomplete cone ERG recovery 20 minutes after a bleach, mice that received the scAAV8-p*RLBP1*(short)-h*RLBP1* vector had a time course of cone recovery that was similar to that observed in *Rlbp1*$^{+/+}$ mice.

AAV-mediated gene transfer of the human *RPE65* gene, which, like *RLBP1*, encodes a protein in the visual cycle, has been used to successfully express *RPE65* in RPE cells and provide long-term recovery of vision in a dog model of Leber congenital amaurosis, type 2 (LCA2) caused by a deficiency of RPE65.[20] The exciting results in the canine study served as the basis for the successful use of the rAAV-*RPE65* vectors in clinical trials of patients with LCA2.[13–15] We are hopeful that a vector like scAAV8-p*RLBP1*(short)-h*RLBP1* that corrects the slow dark adaptation of photoreceptors in *Rlbp1*$^{-/-}$ mice will similarly improve retinal function in patients with *RLBP1*-associated retinitis pigmentosa.

MATERIALS AND METHODS

Assay of the mouse *Rlbp1* gene

Mouse DNA was extracted from submandibular vein blood which was collected into EDTA containing tubes (BD, Franklin Lakes, NJ). DNA was purified using the QIAamp DNA Blood Mini Kit (QIAGEN, Valencia, CA). Oligomer primers P-9 (5′-GCAGTGTTCCCAAAGTATAGC) and P-14 (5′-CTAAGGTGGTCTGAGTACTG) were synthesized and used to amplify both the wild type and KO alleles. In addition, a third oligomer, P3 (5′-GAAGAGCCCAAGATACTCAC), was synthesized and used with P-9 in a confirmatory PCR reaction which would amplify only wild-type sequences. Each PCR reaction was performed in 50 µl containing 2 units of iProof High Fidelity DNA Polymerase (BioRad, Hercules, CA), 1 X iProof HF buffer, 0.6 µmol/l of the 5′ and 3′ primers, 400 µmol/l of each dNTP (dATP, dTTP, dCTP, and dGTP) and 20 ng of DNA. Cycling parameters were as follows: an initial denaturation at 98 °C for 3 minutes followed by an additional 10 seconds at 98 °C, 30 seconds of annealing, and 30 seconds for polymerization at 72 °C. Annealing started at 65 °C and decreased by 1 degree each cycle for 10 cycles. The reaction was completed with an additional 29 cycles including 10 seconds at 98 °C, 30 seconds at 55.6 °C, and 30 seconds at 72 °C, and there was a final polymerization of 72 °C for 2 minutes. The amplicon size for mutant and wild-type alleles using primers P-9 and P-14 are 358 bp and 854 bp respectively. The amplicon size for the wild-type allele using primers P-9 and P-3 is 334 bp and no amplicon is expected for the mutant allele.

Preparation of rAAV8 vector

Six five-layer CellSTACK culture chambers (Corning, Lowell, MA) were seeded with the AAV293 subclone of HEK293 cells (Stratagene, La Jolla, CA) and incubated at 37 °C in 500 ml of DMEM media with 10% FBS. Twenty-four hours postseeding, cells were simultaneously transfected with the following three plasmids: a plasmid containing the transgene expression cassette

flanked by inverted terminal repeat sequences; a plasmid containing the AAV2 replication gene (*Rep2*) and the AAV8 capsid gene (*Cap8*), and finally the adenovirus helper plasmid pHelper.[21] For the triple-plasmid transfection of each CellSTACK, a total of 2.2 mg of DNA at a molar ratio of 2:1:1 ITR-plasmid: *Rep2-Cap8* plasmid: adenovirus helper plasmid (for vectors with a single-stranded genome, a molar ratio of 1:1:1 was used) and 6.6 mg of PEI Max (Polysciences, Warrington, PA) were incubated in 176 ml of OptiMEM for 15 minutes at room temperature. The OptiMEM was then added to 320 ml of DMEM containing 2% FBS. This media was used to replace the media within the cell stacker and cells were incubated at 37 °C at 5% CO_2 for ~90 hours. Cells were removed from the shelves of the cell factories by gently banging the unit against a soft surface and decanted into 500-ml conical centrifuge tubes. Cells were pelleted at 490 × *g* for 15 minutes. The cell pellet was retained in the centrifuge tubes and the supernatant filtered through a 0.2 micron PES filter (Millipore, Billerica, MA).

Vectors in cells as well as in the media were collected and purified as follows. Cell pellets were resuspended in a total of 120 ml of Dulbecco's phosphate buffered saline (dPBS). Aliquots of 10 ml were sonicated with 20 1-second pulses at 50% intensity to lyse cells (Branson Digital Sonifier 250, Danbury, CT). Sonication was repeated four times, with samples incubated on ice in between each round of sonication to avoid overheating. Cell lysates were centrifuged at 3,488 × *g* for 15 minutes. The pellets were discarded and supernatants were collected and pooled. For the filtered media, vectors were precipitated with 3.3% polyethylene glycol (MW 10,000) and 0.2% NaCl incubated for 4 hours at 4 °C (1 hour with mixing and 3 hours without). The precipitated vectors were pelleted by centrifugation at 2985 × *g* for 15 minutes followed by decanting of the media. The precipitated vectors from the media were resuspended with the supernatant collected from the cell lysate and the mixture was incubated with 250 U/ml of Benzonase (EMD Millipore, Billerica, MA) at 37 °C for 45 minutes. Samples were centrifuged at 3,488 x *g* for 15 minutes and the supernatant was retained. The total volume of the sample was adjusted to 120 ml by adding dPBS. Vectors were purified by two rounds of centrifugation in solutions of cesium chloride. Twelve 10-ml aliquots of the lysate were first layered on top of a step gradient consisting of 20 ml of a CsCl solution with a density of 1.2 gm/cm^3 over 5 ml of a solution of CsCl with a density of 1.5 g/cm^3. Following centrifugation at 26,000 rpm in a SW28 Beckman rotor for 75 minutes at 18 °C, 5 ml of fluid at the step density interface was removed from each centrifuge tube by withdrawing through a needle inserted at this interface. Recovered samples were pooled and the concentration of CsCl in the sample was adjusted by adding CsCl and dPBS to yield a refractive index of $1.3722\eta_D \pm 0.0005\eta_D$. This solution was sealed into 13-ml centrifuge tubes and centrifuged at 18 °C overnight at 55,000 rpm in a Beckman NVT-65 rotor to establish a continuous CsCl gradient. From each centrifuge tube, 18–20 0.5-ml aliquots were serially collected by dripping through a 21-gauge needle inserted near the bottom of the centrifuge tube. Fractions with a refractive index of $<1.374\eta_D$ and $>1.368\eta_D$ were dialyzed in dPBS containing 0.001% Pluronic F68 (Invitrogen, Grand Island, NY). Fractions were analyzed for purity by Silver Stain (LC6100; Life Technologies Cat, Grand Island, NY) according to the manufacturer's protocol. Fractions which contained vectors with the least amount of contaminating cellular protein were pooled and concentrated using an Amicon Ultra-4 centrifugation filter unit (Millipore, Billerica, MA) to approximately a 0.5–1 ml volume. The titer of the vector was determined using qPCR that utilized primers and probes located in the SV40 polyadenylation signal sequence as previously reported.[22] Final purity of the concentrated vector was assessed by Silver Stain (LC6100; Life Technologies Cat).

In addition to vectors produced in-house, a limited number of batches of vector were produced by Genethon (Evry Cedex, France) or The University of North Carolina Vector Core (Chapel Hill, NC).

Sequences used in rAAV constructs

The numbering scheme for all promoter sequences is based on the genomic sequence where base 1 is the first base of the initiation methionine codon at the translation start site and the previous nucleotide is base -1. Two versions of the human *RLBP1* promoter were tested. The shorter version (p*RLBP1*(short)) was based on previous promoter activity experiments[23] and was 590 bp in length, extending from nucleotides -3,157 to -2,568 of the human *RLBP1* sequence (NCBI Reference Sequence: NG_008116.1). The longer version (p*RLBP1*(long)) of the human *RLBP1* promoter was 3,157 bp in length and extended from -3,157 bp in the human *RLBP1* sequence to -1 bp including introns 1 and 2.

The *RPE65* promoter sequence contained nucleotides -1,610 through -31 of the human *RPE65* sequence (NCBI Reference Sequence: NG_008472.1. The *BEST1* promoter sequence comprised nucleotides -696 through -74 of the human *BEST1* sequence (NCBI Reference Sequence: NG_009033.1).

The eGFP transgene sequence used in vectors was based on the coding sequence for the enhanced green fluorescent protein gene in the Clonetech cloning vector, pEGFP1 (Genbank:U55761.1). The human *RLBP1* transgene sequence used in the vectors was based on the coding portion of the human *RLBP1* gene mRNA sequence (NCBI Reference Sequence: NM_000326). In all vectors with a transgene, the Kozak consensus sequence, GCCACC, was inserted after the promoter sequence and just upstream of the ATG transcriptional start site of a transgene. The null vector contained a 1,503-bp fragment, extending from nucleotides -2,446 to -944 of intron 1 of the human *RLBP1* gene (NG_008116.1) and a 2,384 bp sequence from the human synuclein alpha gene, including the last 313 bp of intron 2, the full 41 bp of exon 3 and the first 2,027 bp of intron 3 (NCBI Reference Sequence: NG_011851.1). The SV40 intron included just downstream of the promoter, was 157 bp in length and composed of nucleotides 502–561 and 1,410–1,497 of SV40 genomic sequence (NC_001669.1), with a sequence of CGGATCCGG as a connecting sequence between the two fragments. The sequence of the SV40 polyadenylation sequence is composed of 238 bp corresponding to nucleotides 2,774 to 2,537 (reverse strand) of SV40 genomic sequence (NC_001669.1). The modified 5′ inverted terminal repeat sequence used for the self-complementary genome vectors was the same as previously published.[24]

Animals

All mouse studies were approved and governed by the Novartis Institutes for BioMedical Research Institutional Animal Care and Use Committee. *Rlbp1*$^{-/-}$ mice were obtained from Lexicon (The Woodlands, TX) and bred at Taconic Biosciences (Germantown, NY). All mice were homozygous for the Met450 variant of *RPE65*.[25] Sexes were evenly distributed between groups as far as feasible at the time of injection with the exception of the null vector-injected group where only female mice were utilized. The *Rlbp1* locus of each studied Lexicon TF0133 *Rlbp1*$^{-/-}$ *and Rlbp1*$^{+/+}$ mouse was analyzed by PCR to confirm the presence of the mutation.

The nonhuman primate study was performed in the Alcon Research Ltd nonclinical laboratory in accordance with Animal Resources and Research Support standard operating procedures. All Cynomolgus monkeys were obtained from Covance (Alice, TX).

CRALBP staining

Mouse eyes were fixed in 10% neutral buffered formalin for 24 hours at 25 °C and embedded in paraffin using a Tissue-Tek VIP processor with the following protocol: 10 minutes in 70% ethanol, 10 minutes in 80% ethanol, 2 changes of 10 minutes in 95% ethanol, 2 changes of 10 minutes in 100% ethanol, one 10-minutes bath and one 15-minutes bath in 100% xylene, 2 changes of 5 minutes in 58 °C paraffin, and 2 changes of 10 minutes in 58 °C paraffin. Samples were solidified in a base mold. Sections were 5 µm thick.

Sections were placed on glass slides and incubated at 37 °C for 2 hours then deparaffinated and rehydrated by immersing the slides twice for 5 minutes in xylene, twice for 2 minutes in 100% ethanol, 2 minutes in 95% ethanol, 2 minutes in 80% ethanol, and twice for 2 minutes in distilled water. Slides were then immersed in 1.5% H_2O_2 for 15 minutes and washed in distilled water for 5 minutes. Slides were immersed in Vector antigen unmasking solution (Vector Laboratories, Burlingame, CA) and treated in a Digital decloaking (Biocare Medical, Concard, CA) chamber pressure cooker at 120 °C for 30 seconds, 90 °C for 10 seconds, followed by equilibration to 10 °C. Slides were washed for 5 minutes in running water followed by washing with 1× TBST buffer for 5 minutes. Slides were then incubated with diluted blocking serum from Vectastain Elite anti-rabbit ABC kit (Vector Laboratories) for 30 minutes. A 1:4,000 dilution of the anti-CRALBP rabbit polyclonal antibody (15356-1-AP, Proteintech, Chicago, IL) was added and slides were incubated overnight at 4 °C. Following two washes of 5 minutes in TBST buffer, slides were incubated with biotinylated goat anti-rabbit IgG secondary antibody from Vectastain Elite anti-rabbit ABC kit at room temperature for 1 hour. Slides were washed twice in 1× TBST then incubated with Vectastain ABC Reagent for 30 minutes. Slides were washed twice in 1× TBST and incubated for 2.5 minutes in NovaRED solution from the VECTOR NovaRED TM substrate kit for peroxidase (Vector Laboratories). Following two final washes with distilled water, slides were counter-stained with hematoxylin using a Tissue-TeK PrismTM H&E stainer (Sakura, Torrance, CA).

Subretinal injection in mice

Pupils were first dilated with one to two drops of 1% cyclopentolate and one to two drops of 2.5 or 10% phenylephrine. The mouse was subsequently anesthetized using an intraperitoneal injection of either tribromoethanol

(125–250 mg/kg) or a ketamine/xylazine cocktail (100–150/5–10 mg/kg). One or two drops of 0.5% proparacaine were applied to the eye. An incision approximately 0.5 mm in length was made with a micro scalpel 1 mm posterior to the nasal limbus. A blunt-ended needle on a 10 µl Hamilton syringe was inserted through the scleral incision, posterior to the lens, toward the temporal retina until resistance was felt. One microliter of vector (containing 200 µg/ml of sodium fluorescein) was then injected slowly into the subretinal space. The eye was examined and the success of the subretinal injection was confirmed by first flattening the cornea with a glass coverslip then visualizing the fluorescein-containing bleb through the dilated pupil with a Leica M820 F19 Ophthalmic surgical microscope (Zeiss, Heerbrugg, Switzerland) fitted with a Philips E240HM Medical Grade Color Monitor (Philips Healthcare, Andover, MA). Eyes with significant hemorrhage or leakage of vector solution from the subretinal space into the vitreous were excluded from further study. After the procedure, Tobrex (tobramycin ophthalmic ointment 0.3%) (0065-0644-35, Alcon, Fort Worth, TX) was applied to each treated eye and the mouse was allowed to recover from the anesthesia prior to being returned to its cage in the housing room. Approximately 1 week postinjection, images of the fundus were acquired using a spectral domain OCT system (Bioptigen, Morrisville, NC). Eyes with substantial complications from the injection procedure such as unresolved retinal detachments, large hemorrhages, or excessive damage to the retina were excluded from all analysis.

Assay for expression of eGFP

Mice were sacrificed and their eyes were harvested 4 weeks after injection and placed in 4% paraformaldehyde for 2 hours at 25 °C and then in dPBS buffer for 1–3 days at 4 °C. The cornea, lens, and vitreous were removed and discarded while the retina and the posterior eye cup were flat-mounted onto glass slides using Vectashield mounting medium (Vector Laboratories). GFP fluorescence in the retina and RPE was photographed with a Zeiss Imaging system (Zeiss, Thornwood, NY) and quantified using AxioVision Software (Zeiss). After imaging, slides with retinal flatmounts were placed in a 1× dPBS-based buffer with 1% BSA and 0.3% Triton X-100 at 25 °C for 30 minutes and the retinal flatmounts were removed from the slides. The eGFP-positive areas of the retina flatmounts were dissected, embedded in OCT, and cryosectioned. Sections were stained with the following cell-specific primary antibodies: mouse monoclonal anti-CRALBP (1:1,000 dilution; MA1-813; Thermo Fisher Sci, Cambridge, MA), mouse monoclonal anti-GFAP (1:1,000 dilution; SMI-21; Covance Antibody Products, Dedham, MA), and goat polyclonal anti-vimentin (1:100 dilution; sc-7557; SantaCruz, Dallas, TX); rabbit polyclonal anti-blue opsin (1:250 dilution; AB5407; Millipore) and rabbit polyclonal anti-red/green opsin (1:250 dilution; AB5405; Millipore); rabbit polyclonal anti PKCα (1:200 dilution; sc-208; SantaCruz); and mouse monoclonal anti GFAP (1:1,000 dilution; SMI-21; Covance Antibody Products). For each immunocytochemistry stain, slides were air dried at room temperature for one hour, rinsed twice in dPBS + 0.25% TritonX for 15 minutes each, and blocked in 1% BSA + dPBS + 0.25% TritonX for 90 minutes at room temperature. Slides were incubated with the primary antibody diluted in 1% BSA + dPBS + 0.25% TritonX at 4 °C overnight. Slides were equilibrated to room temperature for 30 minutes then washed twice in dPBS + 0.25% Triton for 15 minutes each. Slides were incubated for 90 minutes at room temperature with a 1:800 dilution of one of the following corresponding secondary antibodies: Goat anti-mouse IgG (1:800 dilution; A11005; Invitrogen), goat anti-rat IgG (1:800 dilution; A11007; Invitrogen), or donkey anti-rabbit IgG (1:800 dilution; A21207; Invitrogen). Slides were washed twice in dPBS + 0.25% Triton for 15 minutes then mounted with a coverslip using Vectashield Mounting Medium with DAPI. The images of fluorescence on the slides were captured with a Zeiss LSM 510 confocal microscope and the ZEN version of the Zeiss software. The images allowed assessments of costaining of the cell-specific markers with eGFP.

Subretinal injection in Cynomolgus monkeys

The eyes of the animals used in this study were free of any abnormalities which may interfere with the purposes of the study. The subretinal injections were performed as described elsewhere[26] with the following modifications: instead of using the RetinaJect, a DORC injector (Dutch Ophthalmic, Exeter, NH) was used. 100 µl containing 1×10^9 vector genomes of scAAV8-p*RLBP1*(short)-eGFP were injected. Fundus photography was performed within approximately 30 minutes after injection to document the location of the bleb, which was inferior to the macula of the retina.

Assay for eGFP in eyes of Cynomolgus monkeys

Seventy-one days after subretinal injections, the animals were sacrificed. Eyes were enucleated and fixed in a solution of 4% paraformaldehyde, 20% isopropyl alcohol, and 4% zinc chloride for approximately 24 hours. Following fixation, each eye was cut vertically where the sub-retinal bleb had been, and the bisected eyes were fixed for another 24 hours in the same buffer. The tissue was then embedded in paraffin.

Paraffin sections were immunolabeled with primary rabbit anti-GFP antibody (1:500) (A-11120; Life Technologies) and a rabbit IgG control antibody (1:250, 1 µg/ml) (011-000-003; Jackson ImmunoResearch Laboratories, West Grove, PA). Slides were subsequently incubated with a secondary biotinylated donkey anti-Rabbit IgG antibody (1:400) (711-065-152; Jackson ImmunoResearch Laboratories), followed by a tertiary antibody, streptavidin-peroxidase conjugate (1:1,000) (016-030-084; Jackson ImmunoResearch Laboratories). Slides were then incubated with 3-amino-9-ethylcarbazole (AEC) and a high sensitivity substrate chromogen (K3469; DAKO, Carpinteria, CA), and counter stained with Mayer's hematoxylin and mounted with Fluoromount-G aqueous mounting medium (0100-01; Southern Biotech, Birmingham, AL). Images were taken with a Nikon 90i microscope.

Western blotting to detect CRALBP

Mouse neural retinas were dissected and flash-frozen immediately after enucleation 4 weeks postinjection then stored at −80 °C. Thawed tissue was lysed in 200 µl of RIPA buffer (9806, Cell Signaling Technology, Danvers, MA) with protease and phosphatase inhibitor (5872, Cell Signaling Technology) and then homogenized using a Tissuelyser (Qiagen, Valencia, CA) operated at 30 Hz for 4 minutes. Lysate was centrifuged at 10,000 rpm for 10 minutes at 4 °C and the supernatant was aliquoted into a fresh tube. Lysate was quantified using a Bradford protein assay and normalized to 5 µg/µl using the RIPA buffer. One hundred and thirty-two micrograms of protein was separated by electrophoresis through a NuPAGE Novex 4–12% Bis-Tris gel in 3-(N-morpholino)propanesulfonic acid buffer (Life Technologies). Proteins were transferred to polyvinyl difluoride membranes using an IBlot system (Life Technologies). The membranes were incubated in Licor blocking buffer (Li-Cor Biosciences, Lincoln, NB) overnight at 4 °C. Membranes were washed twice for 5 minutes in dPBS buffer containing 0.05% (v/v) Tween 20 (0.05% PBST) at room temperature then blotted with a 1:100 dilution of mouse monoclonal anti-CRALBP antibody (sc59487, Santa Cruz Biotechnology) for 2 hours at room temperature. The membranes were washed five times for 5 minutes each in 0.05% PBST at room temperature then blotted with a 1:10,000 dilution of donkey anti-mouse secondary antibody (Li-Cor Biosciences, Lincoln, NB) for 1 hour at room temperature. After five washes of 5 minutes each in 0.05% PBST, the membrane was scanned using the Odyssey system imager (Li-Cor Biosciences, Lincoln, NB)

mRNA quantification

Four vectors carrying the human *RLBP1* coding sequence were injected bilaterally to the subretinal space of five WT mouse eyes for a total of 10 eyes per each dose of vector at 1×10^9 vg/eye and 1×10^8 vg/eye, respectively. Five uninjected mice were included in each cohort as negative controls.

Mice were euthanized 4 weeks postinjection and eyes were enucleated. For each eye collected, an incision was made in the cornea and the lens was removed and discarded. The neural retina was dissected out of the eye, placed in a 2-ml round-bottomed polypropylene tubes (990381, Qiagen) and flash-frozen on dry ice. The rest of the eye tissue, which includes the RPE, was placed in a separate 2-ml tube and also flash-frozen. Samples were stored at −80 °C until RNA isolation.

RNA was extracted from the samples using an RNeasy micro kit with DNase treatment (Qiagen). For tissue homogenization a Tissuelyser (Qiagen) was used with a shaking frequency of 30 Hz for 4 minutes. RNA was eluted from the RNeasy micro kit column in 30 µl of RNAse-free water. Each sample was adjusted to a final concentration of 50 ng RNA per microliter with RNase-free water. cDNA was generated from 500 ng of each RNA sample using the Applied Biosystems High Capacity cDNA reverse transcriptase kit (Applied Biosystem at Invitrogen, Grand Island, NY).

Following cDNA synthesis the concentration of each sample was adjusted to a final concentration of 20 ng/µl of the original RNA used in the reverse transcription reaction by adding 5 µl of RNase-free water. Two different multiplex qPCR reactions were performed for each cDNA sample; one using 5 µl of cDNA (100 ng) with the mouse *Rlbp1* Taqman Expression Assay (Applied Biosystems 4331182: Mm00445129.m1) with a mouse GAPDH endogenous

control (Applied Biosystems 4352339E), and the other using 5 µl of cDNA and the human *RLBP1* Taqman Expression Assay (Applied Biosystems 4331182: Hs00165632.m1) with mouse GAPDH endogenous control. qPCR reactions were carried out using an Applied Biosystems 7900HT real-time PCR system. A modified $\Delta\Delta C_t$ method for relative quantitation analysis was applied to determine the expression of human *RLBP1* relative to the endogenous expression of mouse *Rlbp1*. In particular, ΔC_t values were determined first by subtracting the C_t value for h*RLBP1* mRNA minus the C_t value for mouse GAPDH mRNA. Similarly, the C_t value for m*Rlbp1* mRNA minus the C_t value for mouse GAPDH mRNA was calculated for each multiplex reaction. The $\Delta\Delta C_t$ was calculated by subtracting the mouse *Rlbp1* mRNA ΔC_t from the human *RLBP1* mRNA ΔC_t. Relative quantitation (RQ) as a fold change was calculated using the formula $RQ = 2^{-\Delta\Delta Ct}$. The statistical significance of the differences in the levels of vector-mediated mRNA expression compared to uninjected mouse eyes was calculated using a one-way ANOVA with a Dunnett's multicomparison test using GraphPad prism software.

Electroretinography

ERGs were acquired using a commercial ERG system (Diagnosys Espion E^2 with dual Colordome Ganzfeld domes, Diagnosys, Lowell, MA). Prior to recording, pupils were dilated with one or two drops of 1% cyclopentolate and one or two drops of 2.5 or 10% phenylephrine. Mice were subsequently anesthetized with an intraperitoneal injection of a ketamine-xylazine cocktail (100–150/5–10 mg/kg) and one to two drops of 0.5% proparacaine were applied to the eyes. Body temperature was maintained during recording by placing the mice on a warm-water heating pad. ERG traces were recorded using a gold loop contact lens electrode (N30, LKC Technologies, Gaithersburg, MD) referenced to a gold nasopharyngeal electrode placed in the mouth (F-ERG-G, Grass Technologies, Warwick, RI). Stable contact lens electrode hydration was accomplished through continuous application of 0.3% hypromellose drops (GenTeal, Alcon, Fort Worth, TX) through flexible tubing at 300 µl/hour. Electrical ground was provided by a 30-gauge platinum subdermal needle electrode placed near the scapular region (F-E2, Grass Technologies). ERG waveforms were analyzed using a script written for this purpose in MATLAB (Mathworks, Natick, MA).

Dark adaptation

Dark adaptation was assessed in one eye per mouse using an ERG protocol requiring two recording sessions. In one session, the maximum dark-adapted light response of the eye was measured after the animal was kept overnight in the dark in a ventilated, light tight enclosure (Phenome Technologies, Chicago, IL). The a-wave amplitude was measured 5 milliseconds after a 2.7 log scotopic (scot) cd s m^{-2} white light flash from a Xenon bulb; up to three successive flashes were averaged with traces containing artifacts excluded prior to averaging. Dark adaptation was assessed in another session typically occurring within 2 days but never more than 9 days before or after quantification of the maximum dark-adapted light response. For data acquired 2 and 4 weeks postinjection, the interval between recordings was 2 and 3 days, respectively. Mice were again dark-adapted overnight and then subsequently the photopigment was bleached with 16 flashes of 3.7 log scot cd s m^{-2} white light (Xenon) while conscious after the pupils had been dilated with cyclopentolate and phenylephrine. Mice were then returned to the light-proof, dark enclosure and then removed for ERGs 4 hours postbleach. The a-wave amplitude at 5 millisecond postflash was then recorded with the same protocol used to determine the maximum dark adapted a-wave amplitude. The degree of dark adaptation (a-wave recovery) for each eye was the a-wave amplitude 4 hours postbleach divided by its respective maximum dark adapted amplitude. An unpaired *t*-test was used to compare AAV8 vector-treated to naive *Rlbp1*$^{-/-}$ mice (Figure 4d). Recovery of a-wave amplitudes was compared between groups using a one-way analysis of variance with a Newman-Keuls multiple comparisons test (Figures 5 and 6). Each time point was analyzed independently for the longitudinal data in Figure 6.

Cone adaptation measurements

Dark adaptation of cones was evaluated after the animals were kept overnight in the dark in a ventilated, light-tight enclosure, 10 weeks after subretinal injection of vector. First, a baseline cone-driven response was acquired using a paired-flash ERG consisting of a 0.5 log photopic (phot) cd s m^{-2} flash presented 800 milliseconds after a 2.7 log scot cd s m^{-2} rod saturating flash. This flash series was repeated 10 times with 1 second between the onsets of each set of paired flashes. The reported b-wave was the average of the series of up to 10 responses with traces containing artifacts excluded prior to averaging. Anesthetized mice were subsequently exposed to a 1-minute photobleach from a 1200 cd (photopic) white LED background presented in a Ganzfeld dome. Cone function recovery (b-wave amplitude) was then monitored using the same paired-flash protocol at 0, 2.5, 5, 10, 15, and 20 minutes after the bleaching light was extinguished. The mice were kept in the dark between the paired-flash ERG recordings. At each time point, the degree of cone dark adaptation was the b-wave amplitude divided by its respective baseline (prebleach) value. Cone recovery after bleach was assessed within groups using a repeated measures, one-way analysis of variance using a Greenhouse-Geisser correction (sphericity not assumed) with a Dunnett's post-test. Recoveries were referenced to the 0 minute time point within each group. Comparisons between groups were also performed for each time point independently using a one way analysis of variance with a Newman-Keuls multiple comparisons test.

CONFLICT OF INTEREST

All authors were employees of Novartis (Novartis Institutes for BioMedical Research or Alcon Division) at the time the studies were conducted. V.W.C., C.E.B., S.R.P., and T.P.D. are listed as inventors on a patent application related to this work.

ACKNOWLEDGMENTS

Funding of the study was supported by Novartis Institutes for BioMedical Research (NIBR). We are grateful to Natasha Buchanan, Nalini Rangaswamy, Shutong Cao, the study team at the Alcon animal facility, and the animal facility staff at NIBR for their technical assistance. We would like to acknowledge Mitch Brigell, Jens Kurth, Tim MacLachlan and Mark Milton for their contributions to this work. We would also like to thank Kali Stasi, Karen Holopigian, and Dennis Rice for critically reviewing the manuscript. V.W.C., C.E.B., T.P.D., and S.R.P. are listed as inventors on a patent application related to this work.

REFERENCES

1. Daiger, SP, Sullivan, LS and Bowne, SJ (2013). Genes and mutations causing retinitis pigmentosa. *Clin Genet* **84**: 132–141.
2. Maw, MA, Kennedy, B, Knight, A, Bridges, R, Roth, KE, Mani, EJ *et al.* (1997). Mutation of the gene encoding cellular retinaldehyde-binding protein in autosomal recessive retinitis pigmentosa. *Nat Genet* **17**: 198–200.
3. Eichers, ER, Green, JS, Stockton, DW, Jackman, CS, Whelan, J, McNamara, JA *et al.* (2002). Newfoundland rod-cone dystrophy, an early-onset retinal dystrophy, is caused by splice-junction mutations in RLBP1. *Am J Hum Genet* **70**: 955–964.
4. Golovleva, I, Bhattacharya, S, Wu, Z, Shaw, N, Yang, Y, Andrabi, K *et al.* (2003). Disease-causing mutations in the cellular retinaldehyde binding protein tighten and abolish ligand interactions. *J Biol Chem* **278**: 12397–12402.
5. He, X, Lobsiger, J and Stocker, A (2009). Bothnia dystrophy is caused by domino-like rearrangements in cellular retinaldehyde-binding protein mutant R234W. *Proc Natl Acad Sci U S A* **106**: 18545–18550.
6. Burstedt, MS, Sandgren, O, Golovleva, I and Wachtmeister, L (2008). Effects of prolonged dark adaptation in patients with retinitis pigmentosa of Bothnia type: an electrophysiological study. *Doc Ophthalmol* **116**: 193–205.
7. Travis, GH, Golczak, M, Moise, AR and Palczewski, K (2007). Diseases caused by defects in the visual cycle: retinoids as potential therapeutic agents. *Annu Rev Pharmacol Toxicol* **47**: 469–512.
8. Wang, JS and Kefalov, VJ (2009). An alternative pathway mediates the mouse and human cone visual cycle. *Curr Biol* **19**: 1665–1669.
9. Wang, JS and Kefalov, VJ (2011). The cone-specific visual cycle. *Prog Retin Eye Res* **30**: 115–128.
10. Saari, JC, Nawrot, M, Kennedy, BN, Garwin, GG, Hurley, JB, Huang, J *et al.* (2001). Visual cycle impairment in cellular retinaldehyde binding protein (CRALBP) knockout mice results in delayed dark adaptation. *Neuron* **29**: 739–748.
11. Pitz, S and Moll, R (2002). Intermediate-filament expression in ocular tissue. *Prog Retin Eye Res* **21**: 241–262.
12. Bunt-Milam, AH and Saari, JC (1983). Immunocytochemical localization of two retinoid-binding proteins in vertebrate retina. *J Cell Biol* **97**: 703–712.
13. Testa, F, Maguire, AM, Rossi, S, Pierce, EA, Melillo, P, Marshall, K *et al.* (2013). Three-year follow-up after unilateral subretinal delivery of adeno-associated virus in patients with Leber congenital Amaurosis type 2. *Ophthalmology* **120**: 1283–1291.
14. Bainbridge, JW, Smith, AJ, Barker, SS, Robbie, S, Henderson, R, Balaggan, K *et al.* (2008). Effect of gene therapy on visual function in Leber's congenital amaurosis. *N Engl J Med* **358**: 2231–2239.
15. Jacobson, SG, Cideciyan, AV, Ratnakaram, R, Heon, E, Schwartz, SB, Roman, AJ *et al.* (2012). Gene therapy for leber congenital amaurosis caused by RPE65 mutations: safety and efficacy in 15 children and adults followed up to 3 years. *Arch Ophthalmol* **130**: 9–24.

16. Vandenberghe, LH, Bell, P, Maguire, AM, Cearley, CN, Xiao, R, Calcedo, R *et al.* (2011). Dosage thresholds for AAV2 and AAV8 photoreceptor gene therapy in monkey. *Sci Transl Med* **3**: 88ra54.
17. Natkunarajah, M, Trittibach, P, McIntosh, J, Duran, Y, Barker, SE, Smith, AJ *et al.* (2008). Assessment of ocular transduction using single-stranded and self-complementary recombinant adeno-associated virus serotype 2/8. *Gene Ther* **15**: 463–467.
18. Li, H, Poor, S, Bigelow, CE, Choi, VW, Hanks, S, Vrouvlianis, J *et al.* (2013). A comparison of the effects of subretinal injection of scAAV2-CMV-GFP on retinal structure, visual function, and GFP expression by two injectors. *Invest Ophthalmol Vis Sci ARVO E-abstract* **54**: 2740.
19. Kolesnikov, AV, Tang, PH, Parker, RO, Crouch, RK and Kefalov, VJ (2011). The mammalian cone visual cycle promotes rapid M/L-cone pigment regeneration independently of the interphotoreceptor retinoid-binding protein. *J Neurosci* **31**: 7900–7909.
20. Acland, GM, Aguirre, GD, Ray, J, Zhang, Q, Aleman, TS, Cideciyan, AV *et al.* (2001). Gene therapy restores vision in a canine model of childhood blindness. *Nat Genet* **28**: 92–95.
21. Rabinowitz, JE, Rolling, F, Li, C, Conrath, H, Xiao, W, Xiao, X *et al.* (2002). Cross-packaging of a single adeno-associated virus (AAV) type 2 vector genome into multiple AAV serotypes enables transduction with broad specificity. *J Virol* **76**: 791–801.
22. Lock, M, McGorray, S, Auricchio, A, Ayuso, E, Beecham, EJ, Blouin-Tavel, V *et al.* (2010). Characterization of a recombinant adeno-associated virus type 2 Reference Standard Material. *Hum Gene Ther* **21**: 1273–1285.
23. Vogel, JS, Bullen, EC, Teygong, CL and Howard, EW (2007). Identification of the RLBP1 gene promoter. *Invest Ophthalmol Vis Sci* **48**: 3872–3877.
24. McCarty, DM, Fu, H, Monahan, PE, Toulson, CE, Naik, P and Samulski, RJ (2003). Adeno-associated virus terminal repeat (TR) mutant generates self-complementary vectors to overcome the rate-limiting step to transduction in vivo. *Gene Ther* **10**: 2112–2118.
25. Wenzel, A, Reme, CE, Williams, TP, Hafezi, F and Grimm, C (2001). The Rpe65 Leu450Met variation increases retinal resistance against light-induced degeneration by slowing rhodopsin regeneration. *J Neurosci* **21**: 53–58.
26. Nork, TM, Murphy, CJ, Kim, CB, Ver Hoeve, JN, Rasmussen, CA, Miller, PE *et al.* (2012). Functional and anatomic consequences of subretinal dosing in the cynomolgus macaque. *Arch Ophthalmol* **130**: 65–75.